LAWRENCE
LIVERMORE
NATIONAL
LABORATORY

UCRL-TR-235973

Low-Temperature Aging Kinetics of a 15-Year Old Water-Quenched U-6wt.% Nb Alloy

L. Hsiung, J. Zhou

October 30, 2007

Disclaimer

This work performed under the auspices of the U.S. Department of Energy by Lawrence Livermore National Laboratory under Contract DE-AC52-07NA27344.

Low-Temperature Aging Kinetics of a 15-Year Old Water-Quenched U-6wt.% Nb Alloy

Luke Hsiung and Jikou Zhou

Chemistry, Materials, Earth, and Life Sciences Directorate
Material Science and Technology Division

1. Introduction

It is well known that U-6wt.% Nb (U-14at.% Nb) alloy has a microstructure containing martensitic phases supersaturated with Nb that can be obtained by rapid quenching the alloy from γ (bcc)-field solid solution to room temperature. The high cooling rate forces the γ-phase solid solution to transform to variants of the low-temperature α (orthorhombic) phase in which Nb is forced to retain in the supersaturated solid solution. However, the crystal lattice of supersaturated solution formed by rapid quenching is in unstable conditions and is severely distorted since the solubility of Nb in the α phase at room temperature is nearly zero under an equilibrium condition. Two variant phases, a monoclinic distortion of α phase that is designated as α″ martensite and a tetragonal distortion of γ phase that is designated as γ^o phase, can form in the as-quenched alloy, as shown in Fig. 1.

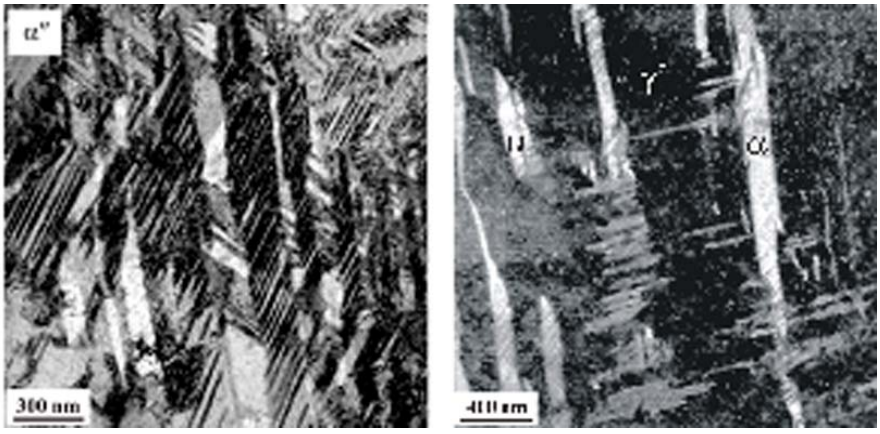

Fig. 1. Bright-field TEM images show the microstructure of a WQ-U6Nb alloy containing both heavily twinned α″ (~90 vol.%) and γ^o (~10 vol.%) martensites.

We have learned from our previous TEM studies on the low-temperature aging of a water-quenched U6Nb (WQ-U6Nb) alloy that there are two possible transformation pathways for phase decomposition of the alloy supersaturated with 14 at.% of Nb upon aging at temperatures below 200°C, i.e., (1) supersaturated solid solution α'' → spinodal decomposition → α_1 (Nb-lean) + α_2 (Nb-rich) at 200°C and (2) supersaturated solid solution α'' → spinodal ordering → α''_{po} (partially ordered phase) → phase decomposition and precipitation → α (U) + α_o (U_3Nb) at ambient temperatures [1]. The mechanisms for the spinodal transformation occurred at 200°C and the spinodal ordering occurred at ambient temperatures are quite similar; both are caused by the composition modulation of Nb except that the wavelength ($\lambda \approx 3$ nm) of modulation for spinodal decomposition is larger than that ($\lambda \approx 0.5$ nm) of modulation for the spinodal ordering, as illustrated in Fig. 2. Since the Nb modulation for the spinodal ordering can occur within the unit cell of α'' phase through the nearest jumps of atoms along the [001] direction, the degree of long-range order (S) increases from 0 to 0.16 as a result of the Nb modulation, as illustrated in Fig. 3. As we accelerated the ordering transformation by thermal heating a 15-year old alloy at 200°C, decomposition of the α''_{po} phase into α (U) and a fully ordered α_o (U_3Nb) phase occured, as shown in Fig. 4. Figure 5 shows the results of microhardness measurement and TEM analysis of the microstructural evolution in the 15-old alloy samples thermally heated at 200°C. Here, it can be clearly seen that the α''_{po} phase with a swirl-shape feature of antiphase boundaries (APBs) vanishes upon heating with the formation of U_3Nb precipitates, which gives rise to the increase of microhardness (precipitation hardening). Figure 6 shows the changes of tensile properties of the 15-old alloy thermally heated at 200°C. It can be readily seen that in addition to the increase of tensile strength (precipitation hardening), the ductility reduces from ~40% to ~14% after heating for 96 hours. In view of these adverse changes in tensile properties upon aging, we accordingly pursued a

precipitation kinetics study on the 15-year old WQ-U6Nb alloy in order to develop an empirical time-temperature-transformation model for predicting the remaining lifetime of the WQ-U6Nb alloy in the stockpile.

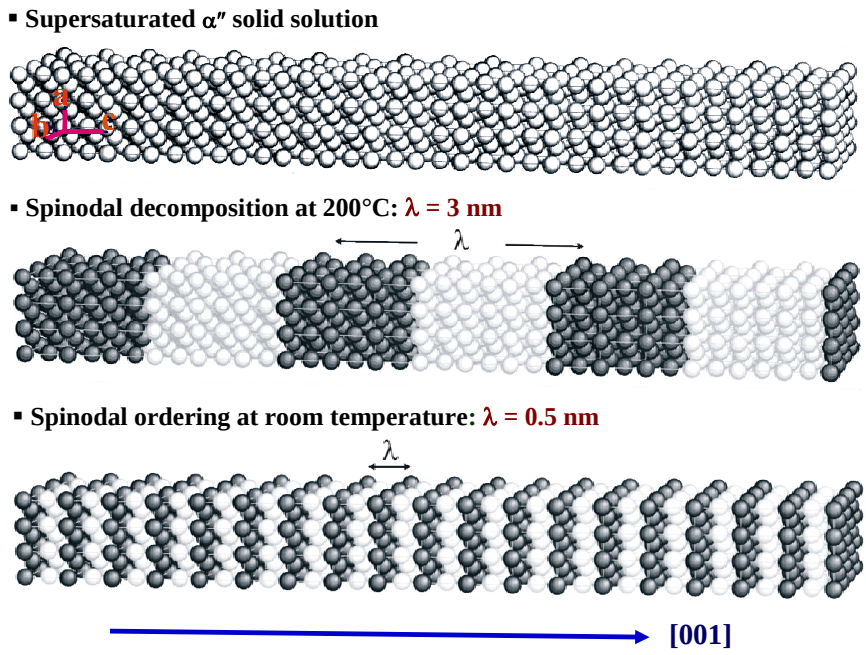

Fig. 2. Schematic illustrations show the temperature dependency of the wavelength of composition modulation, in which the dark spheres represent the Nb-enriched atomic positions.

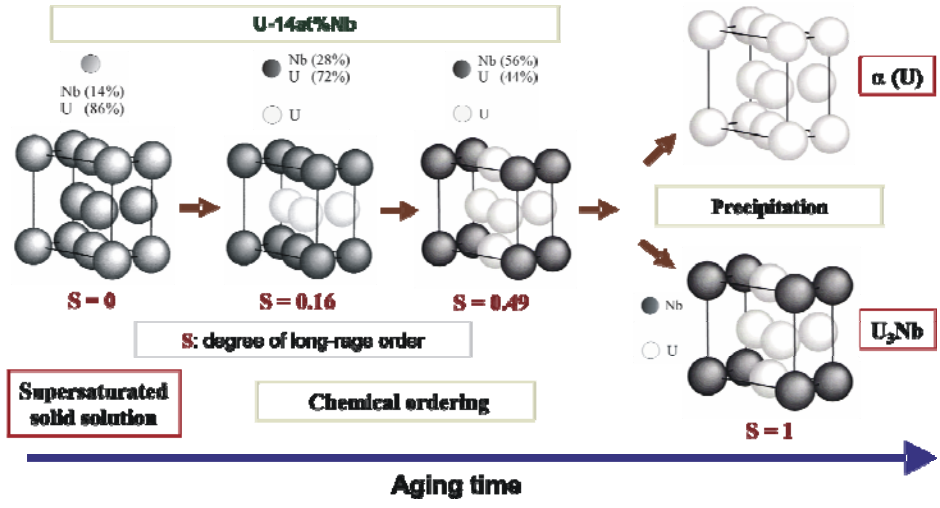

Fig. 3. Schematic illustration of the transformation sequence for an order-disorder transformation in the 15-year old, naturally aged WQ-U6Nb alloy.

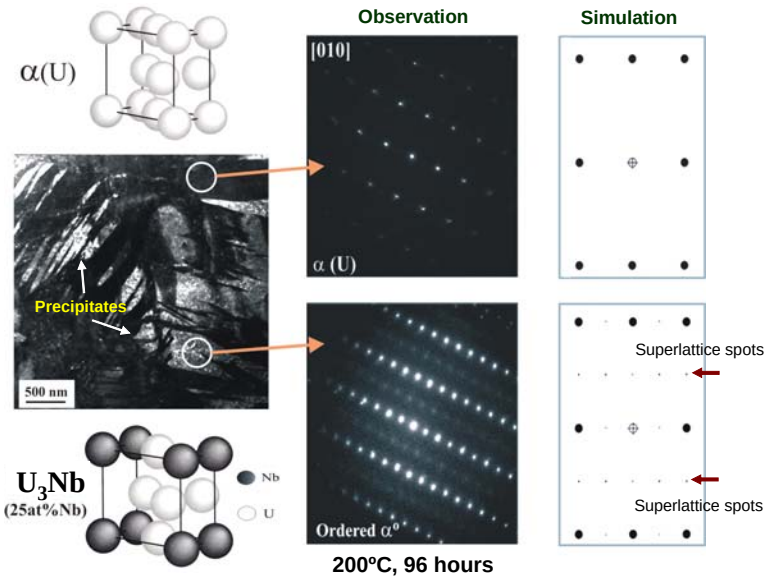

Fig. 4. The partially ordered α_o'' phase decomposes into α (U) and ordered U_3Nb phases, as identified by observed and simulated electron diffraction patterns, when the 15-year old alloy was heated at 200ºC.

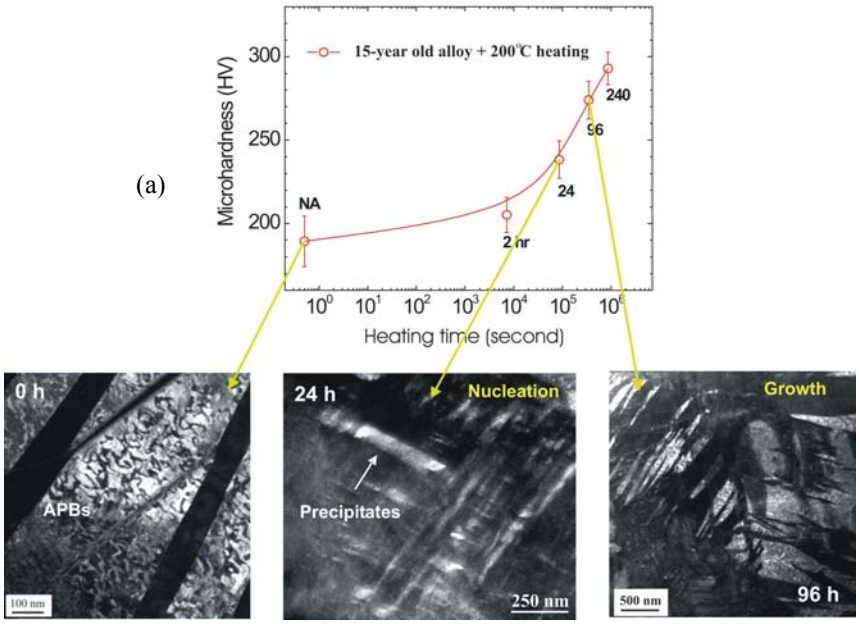

Fig. 5. (a) Precipitation hardening occurred during thermal heating of the 15-year old alloy at 200°C. Dark-field TEM images show (b) APBs in the 15-year old alloy, (c) fine precipitates formed in the alloy after heating for 24 hours, and (d) relatively higher volume fraction of precipitates formed in the alloy after heating for 96 hours. Notice in (c) and (d) that the APBs observed in (a) vanished after aging at 200°C.

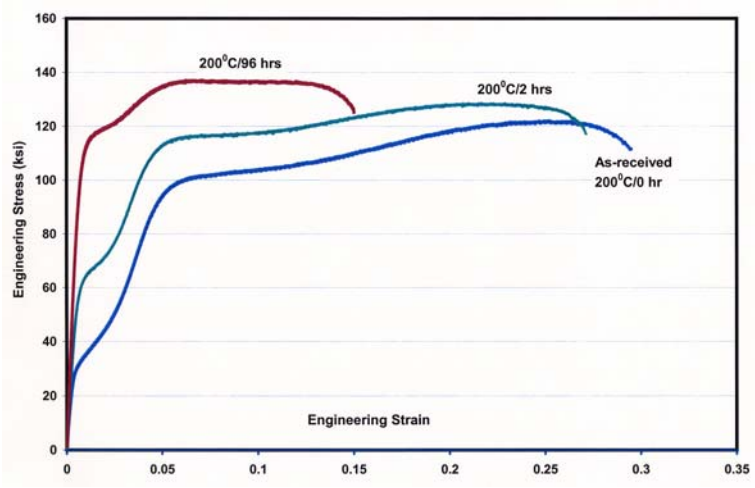

Fig. 6. Thermal aging of the 15-year old WQ-U6Nb at 200°C results in an increase of the yield strength (precipitation hardening) and a significant reduction of the tensile ductility.

2. Experimental approach and methodology

2.1. Precipitation kinetics

The nucleation rate (N^*) of a α_o (U_3Nb) phase formed in the partially ordered α''_{po} matrix can be expressed as: $N^* = n_s \nu_o \rho N_v \exp[-(\Delta G_a + \Delta G_c)/kT]$ (1), where N^* is in units of nuclei per unit volume per unit time, n_s is the number of matrix atoms on the surface of a nucleus, ν_o is the frequency of jumps, ρ is the direction factor of jumps, N_v is the number of atoms per unit volume, k is Boltzman constant, ΔG_a is the activation energy for diffusion, and ΔG_c is the critical energy barrier for nucleation. Let K_v (the frequency factor) = $n_s \nu_o \rho N_v$, thus eqn (1) can be rewritten as: $N^* = K_v \exp[-(\Delta G_a + \Delta G_c)/kT]$ (2).

After a nucleus appears, it can further reduce its free energy by continuous growth. The solute atoms can be transferred by diffusion in several steps: (a) the migration of solute atoms through the parent phase, (b) the migration of solute atoms across the interface boundary, and (c) the migration of solute atoms into the nucleus. For an one-dimensional needle (or plate) growth mechanism, the rate-limiting step is to lengthen the α_o (U_3Nb) plates. Since it is diffusion control, it obeys a parabolic

growth law, and the lengthening of a lath [L(t)] can be expressed as: $L(t) = C \exp[-\Delta G_a/2kT] (t - t_o)^{1/2}$ (3), where C is a constant, and t_o is the instant of time when the nucleus forms.

Nucleation actually continues at all times during the precipitation process. In the time dt_o, $n^* dt_o$ nuclei are formed, where n^* is in units of nuclei per unit time. The total volume (V_T) which has transformed since the beginning of the precipitation (t_o) can be expressed as follows: $V_T = C\, n^* \int (t - t_o)^{1/2}\, dt$ (4). It is noted that the maximum volume of α_o (U_3Nb) precipitates can be reached during the precipitation process is ~56 vol.%; the transformation can be considered to be 100% completed when the maximum vol.% of precipitates is reached. If Y is the percentage transformed, and dx is a fraction of transformed solution from the untransformed solution (1 - Y), then we have (1 - Y) dx = dY (5), where dY is the increment of fraction transformed.

Integrating the above equation, we obtain: $Y = 1 - e^{-x}$ (6), and $x = V_T/V_0 = C (n^*/V_0) \int (t - t_o)^{1/2}\, dt$. Thus, $Y = 1 - \exp[-C N^* \int (t - t_o)^{1/2}\, dt]$ (7). By inserting eqn (3) into (7), it becomes $y = 1 - \exp(-0.5\, C N^*\, t)$ (8), and by inserting eqn (2) into eqn (8), it becomes $Y = 1 - \exp\{C_0 \exp[-(1.5\Delta G_a + \Delta G_c)/kT]\, t\}$ (9). This has the form of Avrami equation [2]: $Y = 1 - \exp(-Kt^n)$ (10) and $K = C_0 \exp[-(\Delta G_a + \Delta G_c)/kT]$ (11), where K is a rate constant that depends on both nucleation and growth rates, and n is a constant that depends on the growth mechanism of precipitate. On the assumption that the time (t) to a given percentage transformed Y (%) is inversely proportional to the rate of nucleation (K), it is possible to write $\ln t = 1.5\Delta G_a/kT + \Delta G_c/kT - \ln C_0$ (12). A schematic representation of the ln t vs. 1/T plot is shown in Fig. 7. By differentiating eqn (12) with respect to 1/T, and since ΔG_a is constant with T but ΔG_c (which decreases with increasing undercooling) is not, it becomes: $d(\ln t)/d(1/T) = 1.5\Delta G_a/k + \Delta G_c/k + [d\Delta G_c/d(1/T)]/kT$ (13).

The percentage transformed, Y(%), can be approximately measured from the change of

microhardness according to law of mixtures: $H_t = H_m V_m + H_p V_p$ and $V_m + V_p = 1$, where, V_m is the volume fraction of matrix, V_p is the volume fraction of precipitate, H_t is the microhardness of transformed alloy, H_m is the microhardness of the alloy without precipitation, and H_p and H_f are the microhardness of the alloy with a specific volume fraction of precipitate and the 100% transformed alloy with $V_p \approx 56\%$, respectively. The microhardness of the transformed alloy increases proportionally with the increasing volume of precipitates and reaches a maximum value when the alloy contains a maximum volume fraction of U_3Nb precipitates; the microhardness starts to decrease when coarsening of the precipitates starts. Thus, the percentage transformed, Y(%), can be approximately evaluated as: $Y(\%) \approx [(H_t - H_0)/(H_f - H_0)]$ (14), where H_t is the hardness of partially transformed material, H_0 and H_f are the values of hardness corresponding to 0% and 100% transformed, respectively.

Since at low temperatures the activation energy for nucleation is small ($\Delta G_c \approx 0$) as a result of large undercooling, thus eqn (13) reduces to $d(\ln t)/d(1/T) \approx 1.5\Delta G_a/k$ (15). That is, the low-temperature part of time-temperature-transformation curve, as schematic illustration shown in Fig. 7, is linear, and the equation for the slope is: $\ln t = 1.5\Delta G_a/kT - \ln C_0$ (16), and $\ln C_0$ is the intercept on the ln t vs. 1/T plot. ΔG_a can therefore be determined from the slope of eqn (16). Given the ΔG_a and C_0 determined by the graphical method, shown in Fig. 7, and a theoretical value of n = 1 [4] for the growth mechanism of needles and plates of finite dimensions, as shown in Fig. 5, the low-temperature kinetics of precipitation reaction in the 15-year old alloy can therefore be modeled using Avrami approach represented by eqn (10).

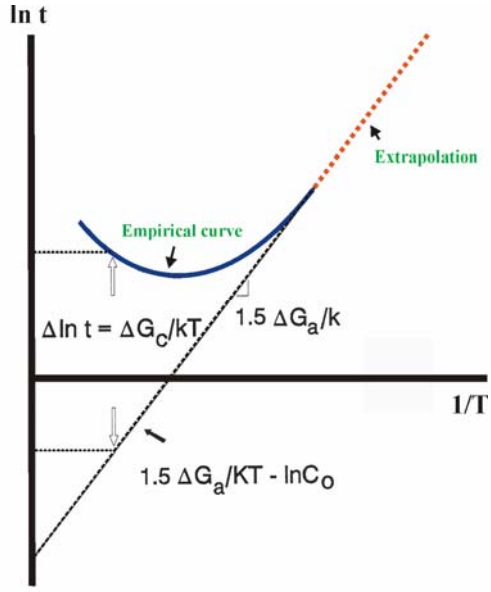

Fig. 7. Graphical meathod of determining the diffusion energy for diffusion (ΔG_a) and activation energy for nucleation (ΔG_c) from an inverse time-temperature-transformation (TTT) diagram.

2.2. Experimental procedure

A stockpile-returned (15-year old) alloy part was employed for the aging kinetics study. The major advantage of employing this alloy part is that the early stages of the precipitation process, i.e., spinodal ordering has been completed. We can therefore focus the study on the precipitation kinetics of the $\alpha''_{po} \rightarrow \alpha$ (U) + α_o (U_3Nb) reaction. Thermal aging experiments (Table 1) were conducted at temperatures ranging between 188°C and 250°C. Microhardness measurements were then carried out to determine the volume fraction of U_3Nb precipitate in the post-aged alloy samples according to eqn (14). The percentage transformed Y(%) of the 15-year old alloy at temperatures below 188°C can therefore be extrapolated from the kinetic model obtained from this study based on eqn (15) by obtaining the value of activation energy for diffusion, ΔG_a, using the graphical method illustrated in Fig. 7.

3. Results and Discussion

Results of microhardness values measured from thermal aging of the 15-year old WQ-U6Nb alloy at 188 °C, 200 °C, 212 °C, 235 °C, and 250 °C are summarized in Table 1. The curves of

microhardness versus aging time are shown in Fig. 8a together with the curve of microhardness obtained from the new WQ-U6Nb alloy thermally aged at 200 °C, which was reported previously [1], for a comparison. These microhardness curves obtained from thermal aging of the 15-year old WQ-U6Nb alloy samples clearly show the dependence of microhardness change on aging temperature. However, it is noted that the peak microhardness value was reached for the aging experiment at 250 °C only since much longer aging periods are required to reach the peak value due to a sluggish kinetics at lower temperatures. The 15-year old WQ-U6Nb alloy sample has a microhardness value of ~190 HV, and the peak microhardness value can be achieved from the heating is ~340 HV.

The thermal aging time (t) required to reach the microhardness value corresponding to the percentage transformaed, Y(%), by 20%, 50%, and 90% are evaluated according to the results of aging experiments that were conducted at temperatures (T) of 200 °C, 212 °C, 235 °C, and 250 °C. It is noted that data obtained from the experiment at 188 °C are not used here since a furnace calibration is in need for the accuracy of the recorded temperature at 188 °C. The results were then re-plotted as ln t versus 1/T, which is shown in Fig. 8b, in which a linear equation with a constant slope but with various intercept values (C) was obtained through line fitting; the equation can be expressed as:

$$\ln t = 11342\frac{1}{T} - C$$

It is noted that the R-Square values for the three fitting lines are greater than 0.98 (a perfect fitting would have a value of unit) suggesting that the fitting is pretty good. For a nucleation-controlled precipitation process, the equation has the following form [2]:

$$\ln t = \frac{\Delta G_a}{RT} - C\,,$$

The activation energy for diffusion (ΔG_a) is evaluated to be 22.5 kcal/mol. However, for a nucleation and growth process, the equation is in the form of eqn (16):

$$\ln t = 1.5\frac{\Delta G_a}{RT} - C\,,$$

The activation energy diffusion is then evaluated to be 15.0 kcal/mol. Accordingly, the aging times required to transform the 15-year old WQ-U6Nb alloy by 20%, 25%, 50%, 80%, and 90% at temperatures 30 °C, 50 °C, 75 °C, and 100 °C can be predicted and are summarized in Table 2 together with a ductility reduction (~65%) measured from an alloy sample transformed by 50%.

Table 1: Microhardness values for heating of the 15-year old WQ-U6Nb alloy.

Aging Temp (°C)	Time (Hr.)	Vickers Microhardness (HV) Average	Std. Dev.
Naturally Aged		**189.4**	**15.2**
188	**2**	**195.8**	**9.2**
	24	**221.0**	**10.7**
	96	**237.3**	**13.4**
	240	**257.1**	**10.2**
	720	**271.2**	**7.4**
	1680	**292.7**	**10.9**
200	**2**	**205.2**	**10.5**
	24	**238.3**	**11.2**
	96	**274.0**	**11.3**
	240	**293.0**	**9.7**
212	**2**	**215.2**	**6.6**
	24	**254.3**	**11.0**
	96	**292.9**	**9.8**
235	**24**	**276.5**	**12.9**
	96	**318.0**	**12.1**
250	**2**	**251.3**	**20.8**
	8	**269.8**	**36.4**
	32	**298.2**	**19.4**
	96	**325.0**	**11.9**
	110	**336.4**	**13.7**
	140	**333.1**	**17.1**

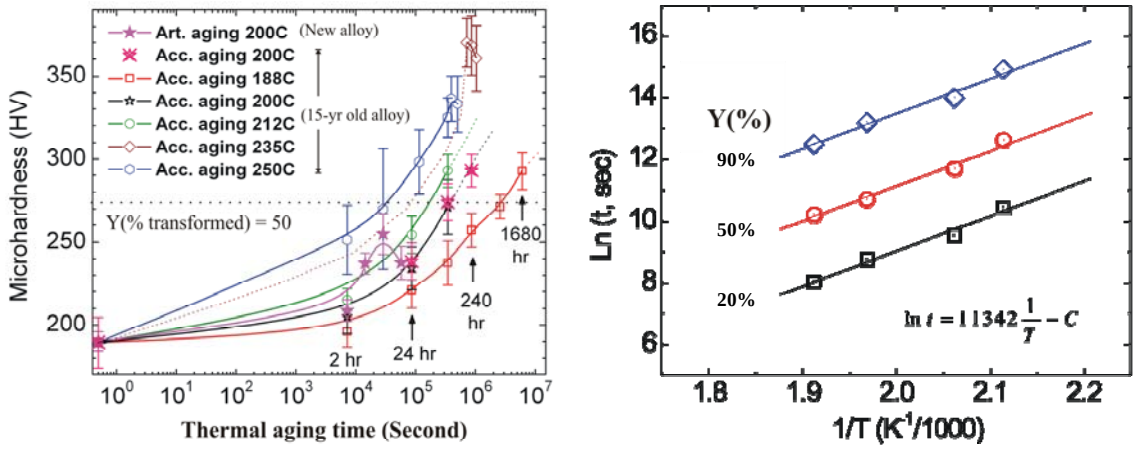

Fig. 8. (a) Microhardness curves obtained from the 15-year old alloys thermally aged at temperatures between 188 °C and 250 °C and (b) a linear equation: $\ln t = 11342\frac{1}{T} - C$ was derived from a ln t vs. 1/T plot for different Y(%).

Table 2 Life-time prediction for the percentage transformed of the 15-year old alloy at temperatures below 100 °C.

Temperature (°C)	Years to be transformed by				
	20%	25%	50%	80%	90%
30	576.1	1095.2	5567.5	29310.6	58000.3
50	57.3	107.9	548.3	2886.8	5712.5
75	4.6	8.7	44.0	231.7	458.4
100	0.5	1.0	5.0	26.1	51.6
Ductility reduction (%)	–	–	~65		

4. Conclusion

Precipitation kinetics of a 15-year old WQ-U6Nb alloy containing partially ordered α''_{po} phase was studied using microhardness measurement of the alloy thermally aged at temperatures between 188 °C and 250 °C in order to develop an empirical time-temperature-transformation model for predicting the remaining lifetime of the WQ-U6Nb alloy in the stockpile. The microhardness increases as a result of the occurrence of decomposition reaction: $\alpha''_{po} \rightarrow \alpha$ (U) + α_o (U_3Nb) during thermal aging of the 15-year old

alloy. The percentage transformed, Y(%), of the alloy was approximately measured from the change of microhardness according to law of mixtures: $H_t = H_m V_m + H_p V_p$ and $V_m + V_p = 1$. The microhardness of the transformed alloy increases proportionally with the increasing volume of precipitates and reaches a maximum value when the alloy contains a maximum volume fraction (~56%) of U_3Nb precipitates; the microhardness starts to decrease when coarsening of the precipitates starts. Thus, the percentage transformed, Y(%), is approximately evaluated as: $Y(\%) \approx [(H_t - H_0)/(H_f - H_0)]$.

The low-temperature kinetics of precipitation reaction were empirically modeled using Avrami equation: $Y = 1 - \exp(-Kt^n)$, and $K = C_0 \exp[-(\Delta G_a + \Delta G_c)/kT]$ together with a graphical meathod to determine the diffusion energy for diffusion (ΔG_a) from an inverse time-temperature-transformation plot. The activation energy diffusion was evaluated to be 22.5 kcal/mol, and the life-time of the 15-year old WQ-U6Nb alloy thermally aged at temperatures below 100 °C were accordingly evaluated.

Acknowledgements

This work was performed under the auspices of the U.S. Department of Energy by Lawrence Livermore National Laboratory under Contract DE-AC52-07NA27344. The authors gratefully acknowledges Dr. T. C. Sun for the work of tensile ductility experiment, Dr. C. Saw for the work of x-ray diffraction analysis, Roger Krueger for the work of aging experiment, Vicki Mason-Reed for the work of optical metallography, and Rick Gross for the preparation of TEM foils.

5. References

1. L. Hsiung and J. Zhou, “Spinodal Decomposition and Order-Disorder Transformation in a Water-Quenched U-6wt.%Nb Alloy,” LLNL Report, UCRL-TR-224432 (2006).

2. J. Burke, "The Kinetics of Phase Transformations in Metals," Pergamon Press, London (1965).

3. M. Avrami, J. Chem. Phys., 7, p. 1103 (1940).

4. J. W. Christian, Chapter 12 in “Transformations in Metals and Alloys,” Pergamon Press, New York , p. 525 (1981).